

Nuclear-Structure Calculations for Cu^{59} and Odd Nickel Isotopes*

R. P. Singh, R. Raj, M. L. Rustgi, and H. W. Kung
*Nuclear Physics Laboratory, Department of Physics and Astronomy,
 State University of New York, Buffalo, New York 14214*

(Received 3 June 1970)

A detailed shell-model calculation is carried out to discuss the properties of the low-lying states of Cu^{59} and Ni^{59} nuclei. An inert Ni^{56} core is assumed and the three extracore particles are considered to occupy the $1p_{3/2}$, $0f_{5/2}$, and $1p_{1/2}$ orbitals. The effect of including the $0g_{9/2}$ orbital is studied. The renormalized reaction matrix elements as derived by Kuo and Brown for this mass region are used. A comparison between the observed and calculated energy levels is made and the wave functions obtained are used to calculate the spectroscopic factors for the $\text{Ni}^{58}(\text{He}^3, d)\text{Cu}^{59}$ and $\text{Ni}^{58}(d, p)\text{Ni}^{59}$ reactions. The odd-mass Ni isotopes (Ni^{59} , Ni^{61} , Ni^{63} , Ni^{65}) are then described by the modified Tamm-Dancoff approximation (MTDA) method. The MTDA results for odd Ni isotopes are found to be in quite satisfactory agreement with experiment. These results together with the previous results for even Ni isotopes by Roy, Raj, and Rustgi lead us to believe that the Kuo-Brown matrix elements in conjunction with the MTDA method give a good description of all the Ni isotopes.

I. INTRODUCTION

In a recent series of publications, Kuo and Brown¹⁻³ have proposed a method for deriving the effective interactions in finite nuclei from the realistic nucleon-nucleon interaction such as the Hamada-Johnston potential. In this method, the excited configurations of the inert core are used to renormalize the matrix elements of the interaction between the active valence nucleons by second- and higher-order terms of the double and multiple scattering type. In the usual shell-model calculations with phenomenological nucleon-nucleon potentials or with adjustable reduced matrix elements to be determined from χ^2 fits to selected pieces of data, the effective forces already include the core-excitation effects. This is not the case with the matrix elements of a "bare" realistic nucleon-nucleon potential. Here an appropriate renormalization for core polarization has to be sought in order to justify a truncation of the single-particle spectrum to allow reasonable maximum dimensions of the Hilbert space for mixing all the important configurations of a given shell-model problem.

Since the publication of the paper by Kuo and Brown (KB), several papers⁴⁻⁶ have appeared which have employed the renormalized KB matrix elements to study the level structure of nuclei in various regions of the Periodic Table. It is found that these matrix elements not only give satisfactory results for some standard nuclear-structure calculations but also provide a good description of nuclei having several nucleons outside a closed core. In a previous publication by Barman Roy, Raj, and Rustgi (BRR),⁷ the KB matrix elements

were employed to study the level structure of even Ni isotopes within the framework of the modified Tamm-Dancoff approximation (MTDA) method. The markedly improved agreement with experimental data has encouraged us to carry out a similar calculation to study the nuclear properties of odd-mass Ni isotopes as well. A calculation on Cu^{59} is of importance because this will test the $T = 0$ matrix elements of KB.

Though the energy levels of Cu^{63} and Cu^{65} have been the subject of several studies, until recently relatively little has been known about Cu^{59} and Cu^{61} . The level structure of Cu^{59} has been recently studied by Pullen and Rosner⁸ by means of the $\text{Ni}^{58}\text{-He}^3, d)\text{Cu}^{59}$ reaction. These authors have extended the measurements on the excited states up to the analog-state region and have compared their results with the unified-model predictions of Bouten and Van Leuven.⁹ The excitation energies of the first four excited states of the odd Cu isotopes are well reproduced by this model. However, no theoretical results have been made available for Cu^{59} on the spectroscopic factors. For other isotopes, in general, the disagreement between theory and experiment is such that the theoretical transition probabilities are larger than the experimental ones; this indicates perhaps that the wave functions of this model contain too large admixtures of shell-model and two-phonon states. Therefore, in this paper a pure shell-model approach is applied. Unlike the calculation of Bouten and Van Leuven, which has three adjustable parameters, the present calculation has none.

In a simple shell-model description of nickel isotopes it is assumed that Ni^{56} closes the $0f_{7/2}$ shell for both protons and neutrons and that the interac-

tion among the valence neutrons gives rise to the observed spectra of these nuclei. Employing this approach and KB renormalized matrix elements for the Hamada-Johnston potential, the shell-model results on Ni isotopes have already been reported by Lawson, MacFarlane, and Kuo⁶ and results for the quasiparticle-approximation have been reported by Gambhir.¹⁰ The renormalized matrix elements used in the present shell-model and quasiparticle calculations also correspond to the Hamada-Johnston potential but are different, as mentioned in BRR.⁷ These matrix elements give markedly improved results in describing the vibrational characteristics of the even Ni isotopes when the calculations are performed within the framework of the quasiparticle method. A theoretical study of 1^+ and 3^+ states in even Ni isotopes has been carried out by Rustgi, Barman Roy, and Raj.¹¹

A major drawback of our calculation, as also of all other similar ones, is that the single-particle energies are not determined in a self-consistent manner. We have taken these energies from the Ni⁵⁷ spectrum. The unperturbed single-particle energy for the $0g_{9/2}$ is not well known and is assumed to be 5.0 MeV as used by Kuo.⁵ It is known that the results of the core-polarization procedure are insensitive to the selection of such a choice. Further, it is found that the results are not very sensitive to large variations in the single-particle energy of the $0g_{9/2}$ orbital.

In Sec. II the results of shell-model calculations of Cu⁵⁹ are reported. In Sec. III similar calculations for Ni⁵⁹ are carried out. In the last section, the odd Ni isotopes are described within the framework of the MTDA method. This method developed earlier^{12,13} and extended recently¹⁴ uses a complete set of orthonormal and nonredundant quasiparticle basis states and describes the levels of odd nuclei as a superposition of one- and three-quasiparticle states.

II. SHELL-MODEL CALCULATIONS FOR Cu⁵⁹

As has been mentioned in the Introduction, the success of the previous calculation by BRR in describing the even Ni isotopes with the KB effective interaction between configurations involving the $1p_{3/2}$, $0f_{5/2}$, $1p_{1/2}$, and $0g_{9/2}$ single-particle orbitals has led us to undertake this extensive calculation for Cu⁵⁹. The method adopted to carry out the calculation consists of computing the shell-model-Hamiltonian matrix between the various allowed configurations for each total spin J and diagonalizing it to find energy levels and wave functions. The wave functions are then used to calculate the spectroscopic factor for the reaction Ni⁵⁸(He³, d)Cu⁵⁹.

As is usual in shell-model calculations, the two-

body reaction matrix elements are fed into the computer as the input data and the shell-model-Hamiltonian matrix employing the expressions listed in Appendix A, is set up. The dimensions of the complete matrices involving all the possible three-nucleon excitations with $1p_{3/2}$, $0f_{5/2}$, and $1p_{1/2}$ orbitals are, respectively, for $J^\pi = \frac{1}{2}^-$, 14×14 ; $\frac{3}{2}^-$, 20×20 ; $\frac{5}{2}^-$, 22×22 ; $\frac{7}{2}^-$, 18×18 ; $\frac{9}{2}^-$, 10×10 ; $\frac{11}{2}^-$, 5×5 ; and $\frac{13}{2}^-$, 2×2 . On including the $0g_{9/2}$ orbital, the dimensions of the matrices range from 1×1 for spin $\frac{23}{2}^-$ to 34×34 for spin $\frac{5}{2}^-$. The unperturbed single-particle energies for the orbitals $1p_{3/2}$, $0f_{5/2}$, and $1p_{1/2}$ were taken to be 0.0, 0.78, and 1.08 MeV, respectively, from the Ni⁵⁷ spectrum. The unperturbed single-particle energy for $0g_{9/2}$ is taken to be 5.0 MeV, as used by Kuo. The effect of varying the single-particle energy for $0g_{9/2}$ to 3.5 MeV is also studied.

The $T=1$ renormalized two-body matrix elements had been already discussed in connection with the previous calculations on even Ni isotopes but the $T=0$ two-body matrix elements did not occur there. These matrix elements have also been calculated by KB and are the sums of three components: the bare interaction uncorrected for polarization of the Ni⁵⁶ core, corrections due to the excitation of a single core nucleon to an empty level, and corrections due to the promotion of a pair of nucleons. A complete discussion of the calculation of these Hamada-Johnston matrix elements can be found in the papers of KB. Though the bare matrix elements have been estimated by KB to be within 15% of the real bare matrix elements, it is difficult to estimate the accuracy of the perturbation corrections or the importance of higher-order terms which have been not included. In the Ni region the perturbative corrections are more important for $T=1$ Hamada-Johnston matrix elements than for those with $T=0$; the correction being about 100% for $T=1$ but only 15% for $T=0$. This, therefore, leads us to believe that the $T=0$ matrix elements will be reasonably close to reality.

In order to perform the numerical work, the computer program employed earlier to generate the three-particle configurations is rewritten so that it can set up the matrix for a given set of single-particle states, total spin, isospin, and parity and then diagonalize it. The program is checked for correctness by reproducing the results of the earlier calculations in which only $T=1$ matrix elements were employed. The energy spectrum for Cu⁵⁹ obtained with KB matrix elements is shown in Fig. 1. In the figure KB3 and KB4 present the results of calculations carried out with three ($1p_{3/2}$, $0f_{5/2}$, $1p_{1/2}$) and four ($1p_{3/2}$, $0f_{5/2}$, $1p_{1/2}$, $0g_{9/2}$) orbitals. As should be expected, the results of KB4 show slightly better agreement with levels whose

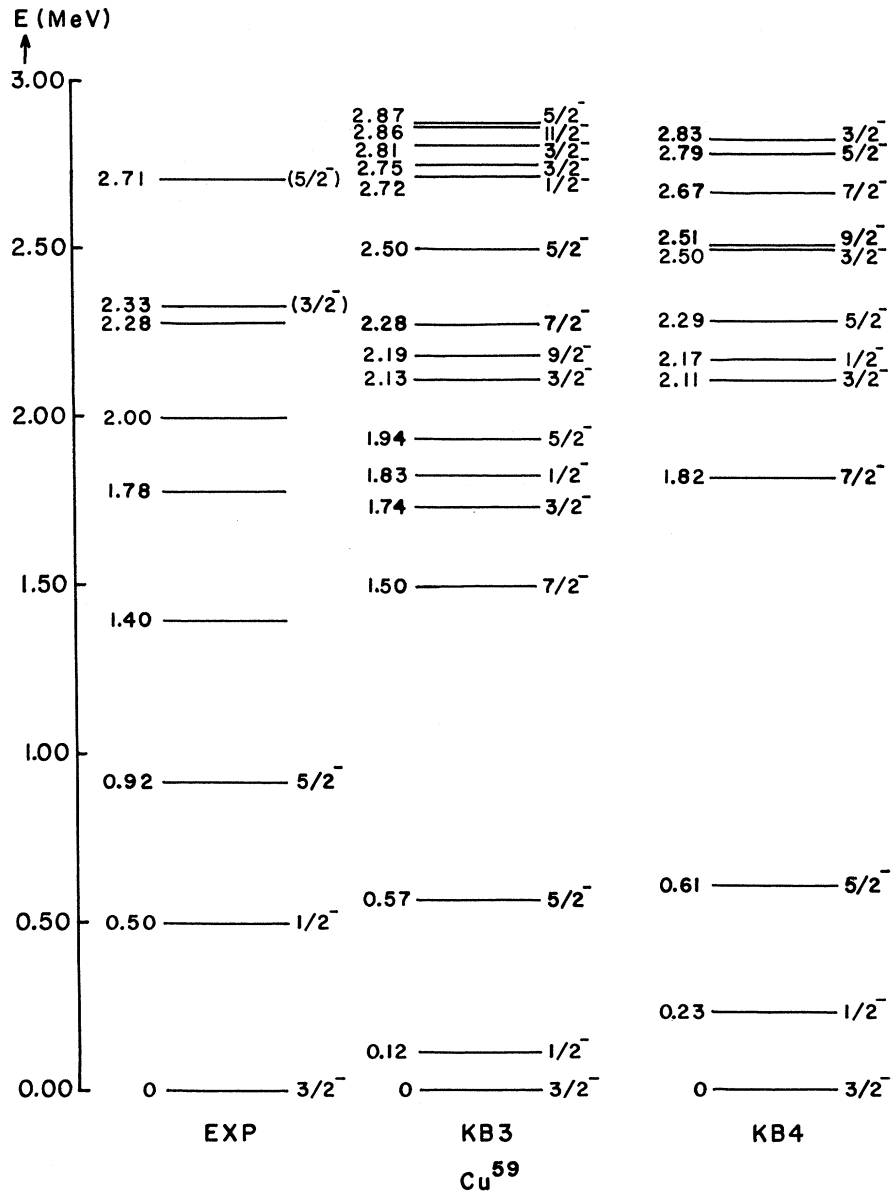


FIG. 1: Comparison of the experimental (EXP) and shell-model spectrum for Cu^{59} . The column labels KB3 and KB4 are explained in Sec. II.

spins are known. The lowest two excited levels calculated theoretically can be perhaps identified with the experimental levels at 0.50 MeV ($\frac{1}{2}^-$), and 0.92 MeV ($\frac{5}{2}^-$). The spins of other levels have not been measured experimentally. The model predicts many more levels than have been observed. The observed levels at 2.33 MeV ($\frac{3}{2}^-$) and 2.71 MeV ($\frac{5}{2}^-$) can perhaps be identified with the calculated levels at 2.50 and 2.79 MeV. The effect of varying the single-particle energy of the $0g_{9/2}$ orbital from 5.0 to 3.50 MeV was found to be insignificant at

least on the first two levels. These levels moved from 0.23 and 0.61 MeV to 0.27 and 0.60 MeV. The higher levels move up on the average by about 0.25 MeV. The lowest levels with $J^\pi = \frac{11}{2}^-, \frac{13}{2}^-, \frac{15}{2}^-, \frac{17}{2}^-, \frac{19}{2}^-, \frac{21}{2}^-,$ and $\frac{23}{2}^-$ occur at 3.23, 3.83, 11.84, 12.57, 12.09, 12.50, and 11.85 MeV, respectively, in the KB4 approximation. When $g_{9/2}$ orbital is excluded, the highest possible allowed $J^\pi = \frac{11}{2}^-$ and $\frac{13}{2}^-$ and their lowest levels exist at 2.86 and 3.47 MeV, respectively.

As a test of the wave functions (listed in Table I)

TABLE I. Lowest energy eigenvalues and eigenfunctions of Cu^{59} . Only amplitudes greater than 0.10 are listed.

Approx.	J^π	Eigenvalues (MeV)	Eigenfunctions
KB4	$\frac{3}{2}^-$	-4.747	$0.63(p_{3/2}^2 01p_{3/2}) - 0.10(f_{5/2}^2 21f_{5/2}) + 0.33(p_{1/2}^2 01p_{3/2})$ $-0.11(p_{1/2}^2 10f_{5/2}) - 0.17(p_{3/2}^2 10p_{1/2}) - 0.19(p_{3/2}^2 21p_{1/2})$ $-0.12(f_{5/2}^2 21p_{1/2}) + 0.53(f_{5/2}^2 01p_{3/2}) + 0.16(f_{5/2}^2 21p_{3/2})$ $-0.17(g_{9/2}^2 01p_{3/2}) - 0.12(p_{1/2} p_{3/2} 20f_{5/2})$
	$\frac{1}{2}^-$	-4.514	$0.23(p_{1/2}^2 01p_{1/2}) + 0.30(p_{3/2}^2 10p_{3/2}) - 0.15(f_{5/2}^2 30f_{5/2})$ $+0.59(p_{3/2}^2 01p_{1/2}) + 0.19(p_{3/2}^2 10p_{1/2}) + 0.25(p_{3/2}^2 21f_{5/2})$ $+0.42(f_{5/2}^2 01p_{1/2}) - 0.15(f_{5/2}^2 10p_{1/2}) + 0.22(f_{5/2}^2 21p_{3/2})$ $-0.13(g_{9/2}^2 01p_{1/2}) + 0.16(p_{1/2} p_{3/2} 20f_{5/2}) - 0.30(p_{1/2} p_{3/2} 21f_{5/2})$
	$\frac{5}{2}^-$	-4.141	$0.52(f_{5/2}^2 01f_{5/2}) + 0.17(p_{1/2}^2 10p_{3/2}) + 0.26(p_{1/2}^2 01f_{5/2})$ $-0.10(p_{1/2}^2 10f_{5/2}) + 0.20(p_{3/2}^2 21p_{1/2}) + 0.55(p_{3/2}^2 01f_{5/2})$ $+0.15(p_{3/2}^2 10f_{5/2}) + 0.23(p_{3/2}^2 21f_{5/2}) + 0.14(f_{5/2}^2 21p_{1/2})$ $-0.12(f_{5/2}^2 30p_{1/2}) + 0.16(f_{5/2}^2 10p_{3/2}) + 0.11(f_{5/2}^2 21p_{3/2})$ $+0.15(f_{5/2}^2 41p_{3/2}) - 0.17(g_{9/2}^2 01f_{5/2}) - 0.21(p_{1/2} p_{3/2} 21f_{5/2})$
KB3	$\frac{3}{2}^-$	-4.354	$0.65(p_{3/2}^2 01p_{3/2}) - 0.11(f_{5/2}^2 21f_{5/2}) + 0.34(p_{1/2}^2 01p_{3/2})$ $-0.12(p_{1/2}^2 10f_{5/2}) - 0.19(p_{3/2}^2 10p_{1/2}) - 0.22(p_{3/2}^2 21p_{1/2})$ $-0.12(f_{5/2}^2 21p_{1/2}) + 0.51(f_{5/2}^2 01p_{3/2}) + 0.10(f_{5/2}^2 10p_{3/2})$ $+0.17(f_{5/2}^2 21p_{3/2}) - 0.13(p_{1/2} p_{3/2} 20f_{5/2})$
	$\frac{1}{2}^-$	-4.230	$0.22(p_{1/2}^2 01p_{1/2}) + 0.33(p_{3/2}^2 10p_{3/2}) - 0.15(f_{5/2}^2 30f_{5/2})$ $+0.60(p_{3/2}^2 01p_{1/2}) + 0.21(p_{3/2}^2 10p_{1/2}) + 0.27(p_{3/2}^2 21f_{5/2})$ $+0.38(f_{5/2}^2 01p_{1/2}) - 0.15(f_{5/2}^2 10p_{1/2}) + 0.22(f_{5/2}^2 21p_{3/2})$ $+0.16(p_{1/2} p_{3/2} 20p_{5/2}) - 0.31(p_{1/2} p_{3/2} 21p_{5/2})$
	$\frac{5}{2}^-$	-3.781	$0.47(f_{5/2}^2 01f_{5/2}) + 0.19(p_{1/2}^2 10p_{3/2}) + 0.26(p_{1/2}^2 01f_{5/2})$ $-0.10(p_{1/2}^2 10f_{5/2}) + 0.24(p_{3/2}^2 21p_{1/2}) + 0.56(p_{3/2}^2 01f_{5/2})$ $+0.17(p_{3/2}^2 10f_{5/2}) + 0.27(p_{3/2}^2 21f_{5/2}) + 0.15(f_{5/2}^2 21p_{1/2})$ $-0.13(f_{5/2}^2 30p_{1/2}) + 0.17(f_{5/2}^2 10p_{3/2}) + 0.11(f_{5/2}^2 21p_{3/2})$ $+0.16(f_{5/2}^2 41p_{3/2}) - 0.23(p_{1/2} p_{3/2} 21f_{5/2})$

obtained in the calculation, the spectroscopic factors for the reaction $\text{Ni}^{58}(\text{He}^3, d)\text{Cu}^{59}$ are also calculated and are listed in Table II. It is found that the calculated spectroscopic factors are in reasonably good agreement with the experimental values. The differences may be partly due to the unreliability of the wave functions, as the agreement for the level spectrum is not complete. The core-excitation model of Lawson and Uretsky¹⁵ also predicts a low-lying quadruplet of states in Cu^{59} with $J^\pi = \frac{1}{2}^-$, $\frac{3}{2}^-$, $\frac{5}{2}^-$, and $\frac{7}{2}^-$ formed by coupling the odd $1p_{3/2}$ proton to the first excited one-phonon 2^+ state in Ni^{58} . In the simplest form of this model these states are not expected to be strongly populated by the (He^3, d) stripping reaction. Bouten and Van

Leuven⁹ have not calculated the spectroscopic factors for the reaction under consideration.

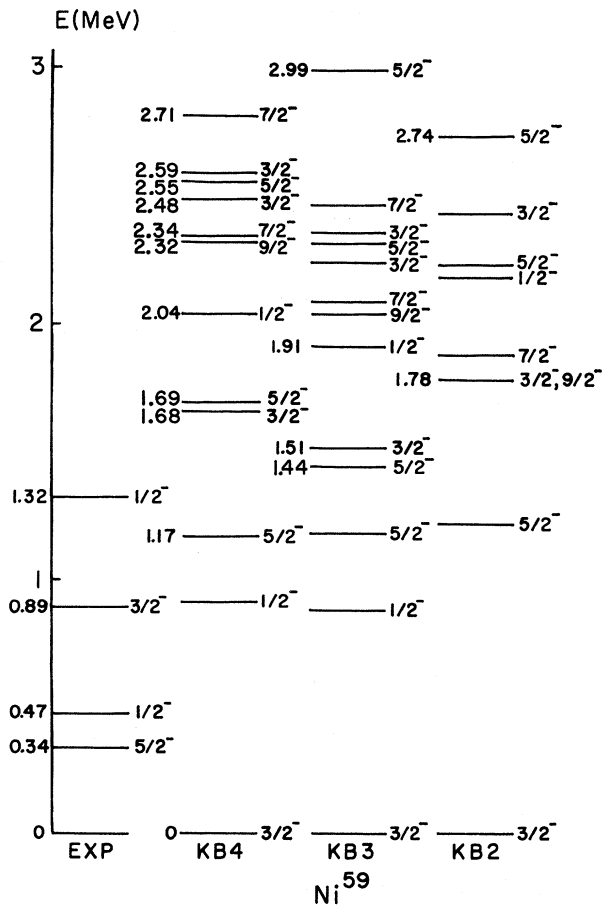
Pullen and Rosner⁸ have identified the levels at 3.904 ($I_p = 1$), 4.315 ($I_p = 3$), and 4.364 MeV ($I_p = 1$) as the $T = \frac{3}{2}$ analogs to the ground ($J^\pi = \frac{3}{2}^-$), 0.341 ($\frac{5}{2}^-$), and 0.466-MeV ($\frac{1}{2}^-$) states in Ni^{59} . In the present calculation these states make their appearances at 2.83 ($\frac{3}{2}^-$), 3.74 ($\frac{1}{2}^-$), and 4.00 MeV ($\frac{5}{2}^-$), respectively. Their spectroscopic factors will be discussed in the next section.

III. SHELL-MODEL CALCULATIONS FOR Ni^{59}

The same procedure as discussed in the previous section is followed to calculate the energy level

TABLE II. Spectroscopic factors for Ni⁵⁸(He³,d)Cu⁵⁹.

J_f^π	$(2J_f+1)C^2S$	$(2J_f+1)C^2S$	
	Expt. (Ref.a)	Without $0g_{9/2}$	With $0g_{9/2}$
$\frac{3}{2}^-$	2.1	3.54	3.64
$\frac{1}{2}^-$	1.1	1.14	1.22
$\frac{5}{2}^-$	4.0	3.79	4.28
$\frac{3}{2}^-$		$<10^{-4}$	$<10^{-4}$
$\frac{1}{2}^-$		0.02	0.03
$\frac{5}{2}^-$		0.18	0.14
$\frac{3}{2}^-$	0.26	0.46	0.39
$\frac{5}{2}^-$	0.12	0.42	0.49

^aSee Ref. 8.FIG. 2. Comparison of the experimental (EXP) and shell-model spectrum for Ni⁵⁹. The column labels KB3 and KB4 are explained in Sec. III. KB2 refers to calculations carried out with two orbitals ($1p_{3/2}$, $0f_{5/2}$).TABLE III. Spectroscopic factors for Ni⁵⁸(d,p)Ni⁵⁹.

J_f^π	$(2J_f+1)S$	$(2J_f+1)S$	
	Expt.	Without $0g_{9/2}$	With $0g_{9/2}$
$\frac{3}{2}^-$	2.77, ^a 2.74 ^b	2.36 ^c	2.52
$\frac{1}{2}^-$	1.24, ^a 1.26 ^b	1.70 ^c	1.46
$\frac{5}{2}^-$	5.19, ^a 4.05 ^b	5.24 ^c	4.69
$\frac{3}{2}^-$			0.26
$\frac{5}{2}^-$			0.50
$\frac{1}{2}^-$			0.33

^aSee Ref. 18.^bSee Ref. 19.^cSee Ref. 19.

spectrum of Ni⁵⁹. For other shell-model calculations, the reader is referred to the papers of Cohen *et al.*¹⁶ and Auerbach.¹⁷ The present calculation is carried out in two approximations. In one approximation the three neutrons outside the Ni⁵⁶ core populate the single-particle orbitals $1p_{3/2}$, $0f_{5/2}$, $1p_{1/2}$. In the second approximation the $0g_{9/2}$ orbit is also included. For $J^\pi = \frac{1}{2}^-, \frac{3}{2}^-, \frac{5}{2}^-, \frac{7}{2}^-, \frac{9}{2}^-$, and $\frac{11}{2}^-$ the dimensions of the matrices to be diagonalized are 5×5 , 10×10 , 10×10 , 6×6 , 5×5 , and 1×1 . When $0g_{9/2}$ is included, the dimensions of the matrices range from 1×1 to 16×16 and the maximum $J^\pi = \frac{21}{2}^-$. The results of the calculations are shown in Fig. 2. It is found that like the previous calculation of Lawson, MacFarlane, and Kuo,⁶ and the BRR⁷ calculation for Ni⁶⁰, this calculation also does not reproduce the correct ordering of the observed levels, though it gives a slightly improved fit to the data over the calculation of Lawson, MacFarlane, and Kuo.⁶ The lowest levels with $J^\pi = \frac{11}{2}^-, \frac{13}{2}^-, \frac{15}{2}^-, \frac{17}{2}^-, \frac{19}{2}^-$, and $\frac{21}{2}^-$ occur at 3.65, 10.95, 11.72, 11.37, 12.29, and 11.46 MeV, respectively, in the KB4 approximation. When the $g_{9/2}$ orbital is excluded the highest allowed spin is $\frac{11}{2}^-$ and its lowest level exists at 3.37 MeV. The variation of the single-particle energy of the $g_{9/2}$ orbital from 5.0 to 3.5 MeV practically has no effect on the lowest levels $J^\pi = \frac{1}{2}^-$ and $\frac{3}{2}^-$, but the levels above 1.5 MeV are moved up on the average by 0.1 MeV.

Table III lists our calculated spectroscopic factors for the reaction Ni⁵⁸(d,p)Ni⁵⁹ together with the experimental data^{18,19} and one other calculation.¹⁶ The calculated spectroscopic factors are in reasonable agreement with the experimental values. This is quite unexpected in view of the fact that the present calculation does not even reproduce the correct ordering and position of the energy levels. This, however, does tell us that the wave functions (list-

TABLE IV. Lowest energy eigenvalues and eigenfunctions on Ni⁵⁹. Only amplitudes greater than 0.10 are listed.

Approx.	J^π	Eigenvalues (MeV)	Eigenfunctions
KB4	$\frac{3}{2}^-$	-1.921	$0.77(p_{3/2}^2 0p_{3/2}) + 0.28(p_{1/2}^2 0p_{3/2})$ $+0.53(f_{5/2}^2 0p_{3/2}) - 0.17(g_{9/2}^2 0p_{3/2})$
	$\frac{1}{2}^-$	-1.009	$0.83(p_{3/2}^2 0p_{1/2}) + 0.17(p_{3/2}^2 2f_{5/2})$ $+0.44(f_{5/2}^2 0p_{1/2}) - 0.16(f_{5/2}^2 2p_{3/2})$ $-0.16(g_{9/2}^2 0p_{1/2}) - 0.17(p_{1/2} p_{3/2} 2f_{5/2})$
	$\frac{5}{2}^-$	-0.753	$0.47(f_{5/2}^2 0f_{5/2}) + 0.27(p_{1/2}^2 0f_{5/2})$ $+0.12(p_{3/2}^2 2p_{1/2}) + 0.80(p_{3/2}^2 0f_{5/2})$ $-0.18(g_{9/2}^2 0f_{5/2})$
KB3	$\frac{3}{2}^-$	-1.603	$0.84(p_{3/2}^2 0p_{3/2}) + 0.26(p_{1/2}^2 0p_{3/2})$ $+0.46(f_{5/2}^2 0p_{3/2})$
	$\frac{1}{2}^-$	-0.725	$0.86(p_{3/2}^2 0p_{1/2}) + 0.23(p_{3/2}^2 2f_{5/2})$ $+0.35(f_{5/2}^2 0p_{1/2}) - 0.21(f_{5/2}^2 2p_{3/2})$ $-0.22(p_{1/2} p_{3/2} 2f_{5/2})$
	$\frac{5}{2}^-$	-0.422	$0.39(f_{5/2}^2 0f_{5/2}) + 0.25(p_{1/2}^2 0f_{5/2})$ $+0.28(p_{3/2}^2 2p_{1/2}) + 0.83(p_{3/2}^2 0f_{5/2})$

ed in Table IV) in the present calculation have almost the right type of admixtures of the various configurations.

IV. QUASIPARTICLE CALCULATIONS FOR ODD Ni ISOTOPES

In order to predict the detailed spectra of odd nickel isotopes, Ni⁵⁹ is assumed to be an inert core and the active neutrons are distributed among the single-particle orbitals $1p_{3/2}$, $0f_{5/2}$, and $1p_{1/2}$, the unperturbed energies of which are listed in Sec. II. The energy spectra of the low-lying states of odd Ni isotopes are described as a superposition of one- and three-quasiparticle states. The detailed method of calculation and all working formulas are given in Ref. 13. Only some of the working formulas are given below. All the notation used here is defined in Ref. 13.

The chemical potential λ and the energy-gap parameter Δ_a are obtained by solving the BCS equations,

$$4\Delta_a = \sum_b \left(\frac{2b+1}{2a+1} \right)^{1/2} \frac{G(aabb0)}{E_b} \Delta_b, \quad (1)$$

and

$$N = \frac{1}{2} \sum_a (2a+1) \left(1 - \frac{\hat{\epsilon}_a - \lambda}{E_a} \right) + \frac{\hat{\epsilon}_j - \lambda}{E_j}. \quad (2)$$

Here, N is the number of neutrons present in the unfilled major shell, $\hat{\epsilon}_a$ is the single-particle energy corrected for self-energy, and $G(aabbJ)$ is the antisymmetric two-body matrix element for total angular momentum J . The quasiparticle energy E_a is given by

$$E_a = [(\hat{\epsilon}_a - \lambda)^2 + \Delta_a^2]^{1/2}. \quad (3)$$

The probability of occupancy V_a^2 and nonoccupancy U_a^2 of a given state a are determined from

$$U_a^2 = \frac{1}{2} [1 + (\hat{\epsilon}_a - \lambda)/E_a], \quad (4)$$

and

$$V_a^2 = \frac{1}{2} [1 - (\hat{\epsilon}_a - \lambda)/E_a]. \quad (5)$$

The energy matrix to be diagonalized may be written as

$$\begin{pmatrix} E & S \\ S & L + E' \end{pmatrix}, \quad (6)$$

where E and E' are the unperturbed energies of one- and three-quasiparticle states, L is the matrix connecting the three-quasiparticle subspaces, while S connects one- and three-quasiparticle subspaces. The explicit expression for the matrices S and L are contained in Ref. 13.

The basic input data required for setting up the energy matrix, beside the two-body matrix elements which in our case are for the Hamada-Johnston nucleon-nucleon interaction, are the quasiparticle energy (E_a), and the occupation probability (V_a^2), which in turn determines the nonoccupation probability $U_a^2 = 1 - V_a^2$, for the single-particle state a . These data are obtained by solving the usual gap and number equations, listed above as (1) and (2), by supplying the pairing matrix elements of the Hamada-Johnston potential. The values of E and V for various single-particle states are listed in Table V. It should be mentioned here that in obtaining the quantities of Table V, the contribution of the extra term arising due to the expectation value of the number operator for a single-quasiparticle state is also included in the number equation.

The effect of the spurious 0^+ pair state from the three-quasiparticle states is eliminated by using a complete set of orthonormal basis states while setting up the energy matrix. Table VI presents the results of such matrix diagonalization for all the odd Ni isotopes and the quasiparticle and experimental spectra are compared in Fig. 3. All the energy eigenvalues up to the first $\frac{5}{2}^-$ state are included. The row MTDA presents results obtained by diagonalizing the energy matrix in the complete space of one- and three-quasiparticle states and the resulting admixture of one-quasiparticle state is represented in row labeled $1qp$. The experimental (Expt.) values are shown for the purpose of comparison. It is to be noticed from this table that for Ni⁵⁹ the shell-model results, presented in the row SM, are not very different from the MTDA results except for the $\frac{5}{2}^-$ states

TABLE V. For each odd Ni nucleus the first row gives the single-quasiparticle energy (E) in MeV and the second row gives the transformation coefficient (V). These are obtained by using the pairing matrix elements of the Hamada-Johnston potential with the extra term in the number equation (mentioned in Sec. IV).

$A \setminus J^\pi$	$\frac{1}{2}^-$	$\frac{3}{2}^-$	$\frac{5}{2}^-$
59	1.81	1.02	1.59
	0.307	0.612	0.371
61	1.58	1.25	1.47
	0.456	0.807	0.552
63	1.32	1.54	1.39
	0.614	0.905	0.719
65	1.11	1.83	1.34
	0.805	0.961	0.868

and do not even reproduce the ordering of the known experimental levels. On the other hand the MTDA results do reproduce at least the ordering of the known experimental levels, although their energies are relatively higher. For Ni⁶¹ the ordering of the first three experimental levels is reproduced within reasonable limits, but our calculation also predicts two more levels below the second $\frac{5}{2}^-$ state, for which experimental information is not known. There is very good agreement for Ni⁶³ between the known experimental and MTDA values. In the case of Ni⁶⁵, the ordering of the first two states is not in agreement, but the next two known levels are reasonably well reproduced.

One can also notice from Table VI that the first state of any given angular momentum is always predominantly of the one-quasiparticle type with the admixture of three-quasiparticle state varying from about 7 to 20%, while the second state is very

TABLE VI. Calculated (MTDA) and experimental (Expt.) energy levels (in MeV) of odd Ni isotopes. All the levels of a given nucleus have been calculated with respect to the lowest of them. The numbers labelled $1qp$ denote the percentage of the one-quasiparticle state. The row SM is the shell-model result for Ni⁵⁹ and is included for the purpose of comparison.

$A \setminus J^\pi$	$\frac{1}{2}^-$	$\frac{1}{2}^-$	$\frac{3}{2}^-$	$\frac{3}{2}^-$	$\frac{3}{2}^-$	$\frac{5}{2}^-$	$\frac{5}{2}^-$	$\frac{5}{2}^-$	$\frac{7}{2}^-$	$\frac{7}{2}^-$	$\frac{9}{2}^-$
59 Expt.	0.47	1.32	0.00	0.89		0.34					
59 SM	0.88	1.91	0.00	1.51		1.18	1.44		2.09		2.04
59 MTDA	0.75	1.78	0.00	1.75	1.97	0.59	1.79		2.08		2.15
59 $1qp$	82.79	10.80	90.00	0.00	3.79	91.62	1.09				
61 Expt.	0.28		0.00			0.07	0.91				
61 MTDA	0.33	1.28	0.00	1.11	1.65	0.28	1.45	1.61	1.52	1.87	1.98
61 $1qp$	83.28	13.04	89.74	2.19	1.72	93.03	0.88	0.52			
63 Expt.	0.00	1.01	0.16	0.53		0.09					
63 MTDA	0.00	1.23	0.18	0.53	1.60	0.08	1.23	1.43	1.32	1.59	1.81
63 $1qp$	89.55	6.52	85.56	4.10	5.34	91.22	3.49	0.03			
65 Expt.	0.06		0.32	0.70		0.00					
65 MTDA	0.00	1.84	0.66	0.87	2.09	0.26	1.61	2.02	1.69	2.09	2.23
65 $1qp$	92.06	2.16	80.05	8.59	2.31	91.95	0.72	0.21			

TABLE VIII. Values of the reduced transition strengths $B(M1)$ and $B(E2)$ for odd Ni isotopes. The column $1qp$ gives the value arising only from the one-quasiparticle component of the MTDA wave functions, and the column MTDA represents the value calculated with the quasiparticle wave functions having also a three-quasiparticle admixture. $B(M1)$ values are in units of μ_N^2 and $B(E2)$ values are in units of $e_{\text{eff}}^2/\alpha^2$ where e_{eff} is the effective charge of the neutron and $\alpha = M\omega/\hbar$ is the harmonic-oscillator parameter.

Reduced transition strength	Ni ⁵⁹		Ni ⁶¹		Ni ⁶³		Ni ⁶⁵	
	$1qp$	MTDA	$1qp$	MTDA	$1qp$	MTDA	$1qp$	MTDA
$B(M1: \frac{1}{2}^- \rightarrow \frac{3}{2}^-)$	1.54	1.80	1.39	1.67	1.42	1.72	1.51	1.88
$B(M1: \frac{3}{2}^- \rightarrow \frac{5}{2}^-)$	0.00	0.0030	0.00	0.0037	0.00	0.0036	0.00	0.0029
$B(E2: \frac{1}{2}^- \rightarrow \frac{3}{2}^-)$	0.76	0.34	0.060	0.022	0.12	0.83	0.88	3.03
$B(E2: \frac{3}{2}^- \rightarrow \frac{5}{2}^-)$	0.10	0.12	0.0009	0.025	0.047	0.015	0.17	0.005

An over-all comparison with other calculations^{10, 13} indicates that the results reported in this paper show better agreement with experiment. These results together with the previous results for even Ni isotopes⁷ indicate that the KB matrix elements give a consistently better description of all the nickel isotopes. It may be desirable to make similar calculations with other realistic potentials such as the Reid potential because of its structural differences from the Hamada-Johnston potential.

ACKNOWLEDGMENTS

Thanks are due the staff of the Computing Center of the State University of New York at Buffalo, which is partially supported by National Institute of Health Grant No. FR-00126 and National Science Foundation No. GP-7318, for providing the machine time. Thanks are also due the Research Foundation of the State University of New York for a grant-in-aid to MLR.

APPENDIX A

For completeness, the matrix elements used in the shell-model calculations of Cu⁵⁹ and Ni⁵⁹ are listed below. The antisymmetric states for the various three-particle configurations are defined by

$$|j_1^3 [J_1 T_1] \nu JT \rangle_a = (-)^{j_1 - J - T - \frac{1}{2}} \sum_{J_1' T_1'} \langle j_1^2 (J_1' T_1'), j_1; JT \rangle |j_1^3 [J_1 T_1] \nu JT \rangle |j_1(3); j_1^2 J_1' T_1'; JT \rangle, \quad (\text{A1})$$

$$|j_1 j_2 J_{12} T_{12}, j_3; JT \rangle_a = \sqrt{\frac{1}{3}} \{ (-)^{j_3 + J_{12} + T_{12} - J - T + \frac{1}{2}} |j_3(3), [j_1(1) j_2(2) J_{12} T_{12}]_a; JT \rangle + \sigma_{j_1 j_2} P(j_1 j_2 J_{12} T_{12}) \times \sum_{J_{23} T_{23}} U(j_1 j_2 J_{23}; J_{12} J_{23}) U(\frac{1}{2} \frac{1}{2} T_{23}; T_{12} T_{23}) |j_1(3), [j_2(1) j_3(2) J_{23} T_{23}]_a; JT \rangle \}, \quad (\text{A2})$$

where

$$P(j_1 j_2 J_{12} T_{12}) + 1 - (-)^{j_1 + j_2 - J_{12} - T_{12} + 1} P(j_1 \leftrightarrow j_2), \quad (\text{A3})$$

$$|j_1(1) j_2(2) J_{12} T_{12} \rangle_a = \frac{1}{\sqrt{2}} \{ |j_1(1) j_2(2) J_{12} T_{12} \rangle - (-)^{j_1 + j_2 - J_{12} - T_{12} + 1} |j_2(1) j_1(2) J_{12} T_{12} \rangle \} \sigma_{j_1 j_2}. \quad (\text{A4})$$

Here J is the total angular momentum, T , the total isospin; ν , the seniority, and the subscripted J and T denote the intermediate coupled angular momentum and isospin. The superscript on j_1 denotes the number of particles present in that particular state and the numbers in the parentheses refer to the particles. The expansion coefficients $\langle \] \rangle$ are the fractional-parentage coefficients. The operator $P(j_1 \leftrightarrow j_2)$ interchanges the subscripts 1 and 2. In Eq. (A1), $(J_1' T_1')$ are the intermediate angular momenta and isospins of the parent state, and $[J_1 T_1]$ are the same for the antisymmetric state for three equivalent particles formed by the above parent state.

With these three-particle basis states, the various matrix elements can be written as

$$\begin{aligned} \langle j_1^3 [J_1 T_1] \nu_1; JT | \sum_{i < k} V_{ik} | j_2^3 [J_2 T_2] \nu_2; JT \rangle_a = 3 \delta_{j_1 j_2} \delta_{\nu_1 \nu_2} \sum_{j_1' T_1'} \langle j_1^2 (J_1' T_1'), j_1; JT | j_1^3 [J_1 T_1] \nu_1; JT \rangle \\ \times \langle j_1^2 (J_1' T_1'), j_1; JT | j_1^3 [J_2 T_2] \nu_2; JT \rangle \langle j_1^2 J_1' T_1' | V_{12} | j_1^2 J_1 T_1 \rangle, \end{aligned} \quad (A5)$$

$$\begin{aligned} \langle j_1^3 [J_1 T_1] \nu; JT | \sum_{i < k} V_{ik} | j_2 j_3 J_{23} T_{23}; j_4; JT \rangle_a \\ = \sqrt{3} \{ \delta_{j_1 j_4} \langle j_1^2 (J_{23} T_{23}), j_1; JT | j_1^3 [J_1 T_1] \nu; JT \rangle \langle j_1^2 J_{23} T_{23} | V_{12} | (j_2 j_3 J_{23} T_{23})_a \rangle + \sigma_{23} P(j_2 j_3 J_{23} T_{23}) \delta_{j_1 j_2} (-)^{j_1 - j - T - \frac{1}{2}} \\ \times \sum_{j_1' T_1'} \langle j_1^2 (J_1' T_1'), j_1; JT | j_1^3 [J_1 T_1] \nu; JT \rangle U(j_2 j_3 J_{23}; J_{23} J_1) U(\frac{1}{2} T_2 \frac{1}{2}; T_{23} T_1) \langle j_1^2 J_1' T_1' | V_{12} | (j_3 j_4 J_1' T_1')_a \rangle \}, \end{aligned} \quad (A6)$$

$$\begin{aligned} \langle j_1 j_2 J_{12} T_{12}; j_3; JT | \sum_{i < k} V_{ik} | j_4 j_5 J_{45} T_{45}; j_6; JT \rangle_a \\ = \delta_{j_3 j_6} \delta_{J_{12} J_{45}} \delta_{T_{12} T_{45}} \langle j_1 j_2 J_{12} T_{12} | V_{12} | j_4 j_5 J_{45} T_{45} \rangle_a + \sigma_{j_1 j_2} P(j_1 j_2 J_{12} T_{12}) \delta_{j_1 j_6} (-)^{j_6 + J_{45} + T_{45} - j - T + \frac{1}{2}} \\ \times U(j_1 j_2 J_{12}; J_{12} J_{45}) U(\frac{1}{2} T_2 \frac{1}{2}; T_{12} T_{45}) \langle j_2 j_3 J_{45} T_{45} | V_{12} | j_4 j_5 J_{45} T_{45} \rangle_a + \sigma_{j_4 j_5} P(j_4 j_5 J_{45} T_{45}) \delta_{j_3 j_4} (-)^{j_4 + J_{12} + T_{12} - j - T + \frac{1}{2}} \\ \times U(j_4 j_5 J_{45}; J_{45} J_{12}) U(\frac{1}{2} T_2 \frac{1}{2}; T_{45} T_{12}) \langle j_1 j_2 J_{12} T_{12} | V_{12} | j_5 j_6 J_{12} T_{12} \rangle_a + \sigma_{j_1 j_2} \sigma_{j_4 j_5} P(j_1 j_2 J_{12} T_{12}) P(j_4 j_5 J_{45} T_{45}) \delta_{j_1 j_4} \\ \times \sum_{J_{23} T_{23}} U(j_1 j_2 J_{12}; J_{12} J_{23}) U(\frac{1}{2} T_2 \frac{1}{2}; T_{12} T_{23}) U(j_4 j_5 J_{45}; J_{45} J_{23}) U(\frac{1}{2} T_2 \frac{1}{2}; T_{45} T_{23}) \langle j_2 j_3 J_{23} T_{23} | V_{12} | j_5 j_6 J_{23} T_{23} \rangle_a, \end{aligned} \quad (A7)$$

where $\sigma_{j_1 j_2} = (1 + \delta_{j_1 j_2})^{-1/2}$.

*Work supported by the U. S. Atomic Energy Commission Contract No. NYO-4022-10.

¹T. T. S. Kuo and G. E. Brown, Nucl. Phys. **85**, 40 (1966).

²T. T. S. Kuo and G. E. Brown, Nucl. Phys. **A92**, 481 (1967).

³T. T. S. Kuo and G. E. Brown, Nucl. Phys. **A114**, 241 (1968).

⁴R. P. Lynch and T. T. S. Kuo, Nucl. Phys. **A95**, 561 (1967).

⁵T. T. S. Kuo, Nucl. Phys. **A90**, 199 (1967), and private communication.

⁶R. D. Lawson, M. H. MacFarlane, and T. T. S. Kuo, Phys. Letters **22**, 168 (1966).

⁷B. Barman Roy, R. Raj, and M. L. Rustgi, Phys. Rev. **C 1**, 207 (1970).

⁸D. J. Pullen and B. Rosner, Phys. Rev. **170**, 1034 (1968). References to earlier experimental papers are given in this publication.

⁹M. Bouten and P. Van Leuven, Nucl. Phys. **32**, 499 (1962).

¹⁰Y. K. Gambhir, Nucl. Phys. **A120**, 193 (1968).

¹¹M. L. Rustgi, B. Barman Roy, and R. Raj, Phys. Rev. **C 1**, 1138 (1970).

¹²P. L. Ottaviani, M. Savoia, J. Sawicki, and A. Tomasini, Phys. Rev. **153**, 1138 (1967).

¹³M. K. Pal, Y. K. Gambhir, and R. Raj, Phys. Rev. **155**, 1144 (1967); Y. K. Gambhir, R. Raj, and M. K. Pal, *ibid.* **162**, 1139 (1967).

¹⁴R. Raj and M. L. Rustgi, Phys. Rev. **178**, 1556 (1969).

¹⁵R. D. Lawson and J. L. Uretsky, Phys. Rev. **108**, 1300 (1957).

¹⁶S. Cohen, R. D. Lawson, M. H. MacFarlane, S. Pandya, and M. Soga, Phys. Rev. **160**, 903 (1967).

¹⁷N. Auerbach, Phys. Rev. **163**, 1203 (1967).

¹⁸R. H. Fulmer, A. L. McCarthy, B. L. Cohen, and R. Middleton, Phys. Rev. **133**, B955 (1963); R. H. Fulmer and W. Daehmick, *ibid.* **139**, B579 (1965).

¹⁹E. R. Cosman, C. H. Paris, A. Sperduto, and H. A. Enge, Phys. Rev. **142**, 673 (1966); E. R. Cosman, D. M. Schramm, H. A. Enge, A. Sperduto, and C. H. Paris, *ibid.* **163**, 1134 (1967).